Hindawi Publishing Corporation
International Journal of Aerospace Engineering
Volume 2016, Article ID 3570581, 11 pages
http://dx.doi.org/10.1155/2016/3570581

Research Article

Preliminary Design of a Small Unmanned Battery Powered Tailsitter

Bo Wang, Zhongxi Hou, Zhaowei Liu, Qingyang Chen, and Xiongfeng Zhu

College of Aerospace Science and Technology, National University of Defense Technology, Changsha 410073, China

Correspondence should be addressed to Zhongxi Hou; nudtxiaowang@163.com

Received 8 November 2015; Revised 4 April 2016; Accepted 17 April 2016

Academic Editor: Paolo Tortora

This paper presents a preliminary design methodology for small unmanned battery powered tailsitters. Subsystem models, including takeoff weight, power and energy consumption models, and battery discharge model, were investigated, respectively. Feasible design space was given by simulation with mission and weight constraints, while the influences of wing loading and battery ratio were analyzed. Case study was carried out according to the design process, and the results were validated by previous designs. The design methodology can be used to determine key parameters and make necessary preparations for detailed design and vehicle realization of small battery powered tailsitters.

1. Introduction

Application Prospects of Battery Powered Tailsitters. A tailsitter has the capabilities of vertical takeoff and landing (VTOL), hover like a helicopter, transition between vertical flight and level flight, and efficient wing-borne flight as a fixed wing aircraft. Designed for reconnaissance, surveillance, delivering, and rescuing, tailsitters could vertically take off from confined environments, such as woodland, small islands, streets, disaster scene, and even mobile platforms on vehicles and ships. The Project Wing [1] of Google X intends to develop tailsitters for rapid package delivery in a wide range of situations, such as delivering defibrillators to heart attack victims in the countryside; the Small Business Innovation Research (SBIR) plan (2012) of the US Air Force aims for a ducted fan powered tailsitter with long endurance.

Powered by batteries and brushless direct current (BLDC) motors, small unmanned tailsitters take the advantages of light weight, low cost, ease of use and maintenance, and low level of vibration and noise. What is more, battery powered tailsitters could take off from the surfaces of Mars and Titan without the help of any runways or launch equipment and then carry out long range exploration, hover on target points, or land directly for detailed detecting. The Surrey Space Centre [2] and the NASA Ames Research Center [3, 4] have studied on such explorer for better mobility and mission performance in Martian exploration.

Design Methodology Review. There are many existing configurations of battery powered tailsitters, such as the Martian tailsitter [2] developed by the University of Surrey, the T-wing [5] and Bidule [6] developed by the University of Sydney, the ITU-Tailsitter [7] developed by Istanbul Technical University, the Japanese SkyEyeV [8], the ATOMS [9] developed by Delft University of Technology, and the Quadshot [10] developed by Transition Robotics. Within these vehicles, only the design methods and processes of T-wing, Surrey Martian tailsitter, and ITU-Tailsitter could be found by open literatures.

Both electrical motor and reciprocating engine had ever been adopted in the development of T-wing unmanned aerial vehicle (UAV), while the battery powered propulsion system was utilized in the early validation phase [5]. The T-wing configuration with a canard and dual propellers was investigated by multidisciplinary optimization based on detailed subsystems, including aerodynamics-propulsion integrated model, weight and structure model, and control model. Such method was efficient for the design of battery powered tailsitter with different missions and constraints when there was little statistical guidance [11]. However, too many parameters and constraints, at least 13 equality constraints,

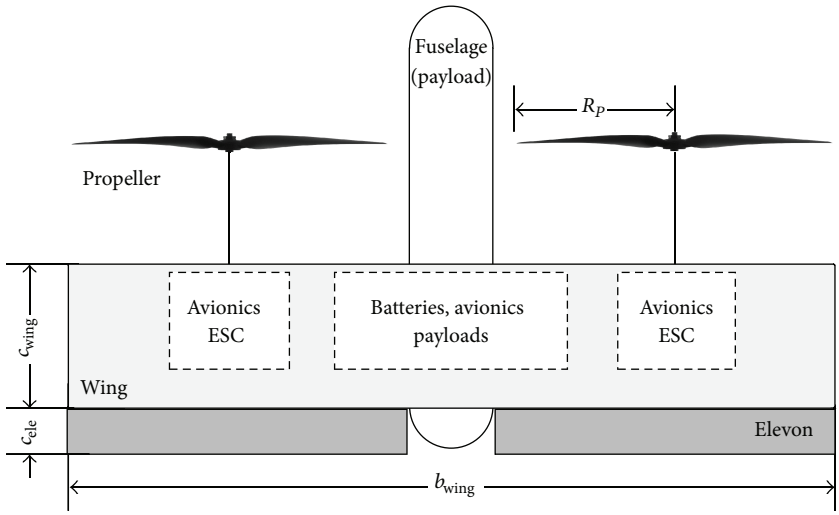

Figure 1: Schematic of a small unmanned battery powered tailsitter.

36 actual design variables, and 75 fixed design parameters, should be taken into consideration. Meanwhile, the feasible design space and the influence of key parameters, such as the ratio of battery weight to takeoff weight (battery ratio), on aircraft performance have not been discussed. A more general tailsitter configuration with twin rotors needs to be studied.

The Surrey Martian tailsitter was an adaption version of QinetiQ's terrestrial Eye-On, which was a "helicopter assembly" twin rotor design [2]. For this tailsitter, twelve disparate critical subsystems were detailedly designed according to the mission architecture and system requirements. High-level balance of mass and power demonstrates the feasibility of the tailsitter. This design method was well illustrated and more likely to be realized by engineers, while the tailsitter's range and endurance performance could be improved if an integrated optimization was implemented.

The ITU-Tailsitter utilized a hybrid-dual propulsion system [7], which was driven by a large diameter folding propeller located on the nose of the aircraft and a small diameter ducted fan system located on the tail of the aircraft. The former was used in the phase of hover, vertical takeoff, vertical landing, and low speed transition, while the latter was used in the phase of level and high speed flight. This is a novel attempt to deal with the efficiency problem of tailsitters, though some dead weight was introduced for each phase. Variables, such as maximum takeoff weight, wing loading, and battery weight, were optimized for maximum payload and cruise duration. Such method could be suitable for the circumstance that the propulsion propeller and ducted fan have been selected. Generally, for preliminary design, neither the propeller diameter nor the thrust function about propeller speed n and airspeed v as $T = T(n, v)$ has been determined. So the optimization design could not go on successfully.

About the Tailsitter. The simplified aerodynamic configuration of battery powered tailsitter consists of four main parts, as shown in Figure 1, fuselage, straight rectangular wing, twin contrarotation propellers, and twin elevons located on the trailing edge. Batteries, payloads, avionics, and other necessary instruments could be contained in the fuselage and the wing.

In order to utilize the propellers' slipstream sufficiently for adequate control moment while attentions should be paid to propellers' low speed vertical flight performance, a propeller radius of $R_P \approx b_{\text{wing}}/4$ was recommended. And variable pitch propellers are proposed for different flight modes, including low speed but high thrust vertical flight mode and high speed but low thrust level flight mode.

The same as Bidule [6], twin elevons were utilized to provide roll-attitude and pitch-attitude control, while rotation speeds and collective pitches of such twin propellers were utilized to provide altitude and yaw-attitude control, respectively. The stability and controllability of such configuration have been validated by Bidule's flight experiments, which will not be discussed here anymore. This paper will focus on weight, power, energy consumption, and endurance performance.

The mission profile of a tailsitter was depicted by dashed lines in Figure 2. The tailsitter climbs vertically from the takeoff point until reaching the mission height and then transits to horizontal flight (V2H); having accomplished the flight mission, the tailsitter will move to the target landing area and transit to vertical descent (H2V) until landing on the ground.

Compared with conventional takeoff and landing (CTOL) aircraft's mission profile, as real lines portrayed in Figure 2, there is no horizontal speedup or slowdown for tailsitters. Each transition on the flight path of the tailsitter was simplified to be along with a right angle for preliminary design. However, an optimized curve transition path should be introduced for actual flight in further study.

Aims and Paper Structure. This paper aims for a feasible solution for the preliminary design of small battery powered tailsitters, which could provide effective guidance about weight, geometry, power, and energy consumption for further detailed design and vehicle realization.

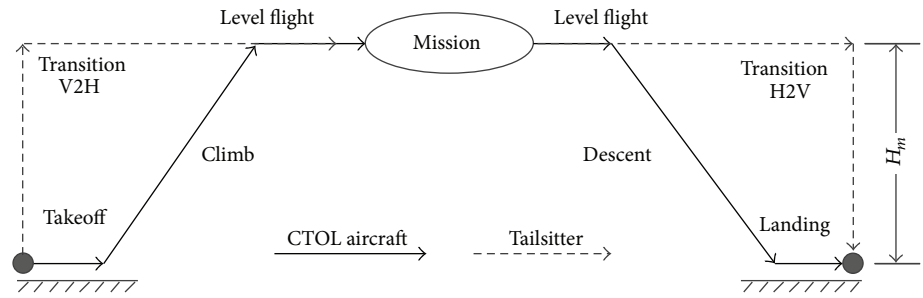

Figure 2: Mission profile comparison between CTOL aircraft and tailsitters.

A small battery powered tailsitter will be designed with current technology to accomplish the flight mission at the height of 1000 m as shown in Figure 2. The allowable mass of the tailsitter is 10 kg, and the mass of the payload is 1.0 kg. The maximum level flight duration will be estimated and the corresponding optimum wing loading and battery ratio will be recommended by optimization.

In Section 2, three subsystems will be modeled, including takeoff weight, power level and energy consumption, and battery discharge. In Section 3, influences of wing loading and battery ratio will be analyzed, and the feasible design space for small battery powered tailsitters will be given. Section 4 will illustrate the preliminary design method and carry out a design case study for validation.

2. Subsystem Models

2.1. Takeoff Weight. Referring to electrically powered rotary-wing platform [12], takeoff weight of an unmanned battery powered tailsitter W_{TO} is composed of four main components: airframe, BEMP propulsion system, avionics, and payloads. The BEMP system consists of batteries, electronic speed controllers (ESCs), motors, and propellers:

$$\begin{aligned} W_{\mathrm{TO}} &= W_{\mathrm{airframe}} + W_{\mathrm{BEMP}} + W_{\mathrm{avionics}} + W_{\mathrm{PL}} \\ &= \underline{W_{\text{fu-str}} + W_{\mathrm{wing}}} + \underline{W_B + W_{\mathrm{EMP}}} + W_{\mathrm{avionics}} \\ &\quad + W_{\mathrm{PL}}, \end{aligned} \tag{1}$$

where $W_{\text{fu-str}}$ represents the integrated weights of fuselage, joint structure, and tailsitter's other structures except wing, W_{EMP} represents the integrated weight of ESC, motor, and propeller, and W_{PL} represents the weight of payloads. The wing weight W_{wing} and battery weight W_B are listed to be discussed individually as they are more significant for aircraft's endurance performance and share a main proportion of the takeoff weight.

Serial weight ratios could be defined: $k_F = W_{\text{fu-str}}/W_{\mathrm{TO}}$, $k_A = W_{\mathrm{avionics}}/W_{\mathrm{TO}}$, and battery ratio $k_B = W_B/W_{\mathrm{TO}}$. The wing weight could be expressed as $W_{\mathrm{wing}} = k_W S$, where S is the wing area and k_W is the wing weight coefficient representing the weight per unit area of the wing in N/m^2. The wing weight could also be expressed by W_{TO}:

$$W_{\mathrm{wing}} = \frac{k_W}{W_{\mathrm{TO}}/S} W_{\mathrm{TO}} = \frac{k_W}{k_{WS}} W_{\mathrm{TO}}, \tag{2}$$

where $k_{WS} = W_{\mathrm{TO}}/S$ represents the tailsitter's wing loading in N/m^2. And then (1) could be simplified as

$$W_{\mathrm{TO}} = W_{\mathrm{EMP}} + \left(\frac{k_W}{k_{WS}} + k_B + k_F + k_A \right) W_{\mathrm{TO}} + W_{\mathrm{PL}}. \tag{3}$$

Solving (3) yields the takeoff weight as

$$W_{\mathrm{TO}} = \frac{W_{\mathrm{EMP}} + W_{\mathrm{PL}}}{1 - k_B - k_A - k_F - k_W/k_{WS}}, \tag{4}$$

where the weight of payloads W_{PL} will be given by mission; W_{EMP} should be determined by the maximum operation power of vertical climb phase. As can be seen from (4), the takeoff weight will increase as k_{WS} decreases or k_B increases for given payloads, when $k_B + k_W/k_{WS} < 1 - k_A - k_F$ is still satisfied.

2.2. Power and Energy. In order to realize vertical takeoff and landing, for tailsitters, the ratio of thrust to weight K_T needs to be greater than one. The maximum design thrust of the tailsitter can be written as

$$T_{\max} = K_T W_{\mathrm{TO}}. \tag{5}$$

Stone [11] suggests that the maximum thrust needs to be 1.15 or higher times greater than takeoff weight, for dealing with nonideal conditions and transition maneuvers. Then a value of $K_T = 1.2$ is proposed for small battery powered tailsitters in this paper.

The required power of a propeller supplied a thrust T for the aircraft which can be calculated by the momentum theory as [13]

$$P(T, V) = \frac{\kappa T V}{2} \left[1 + \sqrt{1 + \frac{2T}{\rho A V^2}} \right], \tag{6}$$

where $A = \pi R_P^2$ is the area of propeller disk; V is the axial forward velocity of the propeller; the induced power factor κ has a typical value in the range of [1.15, 1.25] and a conservative value $\kappa = 1.2$ was suggested. Although the momentum analysis can not give a precise result for power calculation, it takes the propeller's efficiency about the thrust and the airspeed into consideration and provides an efficient solution for preliminary design without the need of propeller's detailed parameters.

2.2.1. Accelerating Climb. For vertical takeoff, the climb velocity will gradually increase from zero under the force of propeller thrust T ($0 < T < T_{\max}$). Having gained the expected climb velocity V_C ($0 < V_C < V_{\max}$), the tailsitter will climb to the mission height with the constant velocity.

Supposing that the accelerating was performed by the allowable maximum thrust $T_{\max}$, the tailsitter reaches height $H(t)$ and the climb velocity is $V(t)$ at time t. Ignoring wing-propeller interaction, forces acting on the aircraft include gravity, propeller thrust, and aerodynamic drag of the wing. It can be deduced by Newton's second law that

$$\sum F_j = T - W_{\mathrm{TO}} - \frac{\rho S C_{D0}}{2} V^2 = m \frac{d^2 H}{dt^2}, \tag{7}$$

where $m = W_{\mathrm{TO}}/g$ is the mass of the tailsitter, ρ is the air density, and C_{D0} is the wing's zero-lift drag coefficient. According to the relationship between displacement and velocity, (7) can be converted into

$$\frac{dV}{dt} = \frac{d^2 H}{dt^2} = \left(k_T - 1\right) g - \frac{\rho S C_{D0}}{2m} V^2. \tag{8}$$

Combined with the initial climb velocity, (8) can be written as

$$\begin{gathered} \frac{dV}{(a/b)^2 - V^2} = b^2 dt, \\ a = \sqrt{g\left(k_T - 1\right)},\ V(t=0) = 0,\ b = \sqrt{\frac{\rho S C_{D0}}{2m}}. \end{gathered} \tag{9}$$

Simultaneous integral on both sides of the differential equation in (9) yields

$$t = \frac{1}{2ab} \ln \left| \frac{a/b + V}{a/b - V} \right| = \frac{1}{2ab} \ln \left| 1 + \frac{2}{a/(bV) - 1} \right|. \tag{10}$$

Referring to the actual situation, the feasible solution of climb velocity about time is

$$V(t) = \frac{a}{b} \frac{\exp(2abt) - 1}{\exp(2abt) + 1}, \quad t \in [0, t_{AC}], \tag{11}$$

where the duration of accelerating climb t_{AC} depends on the expected constant climb velocity V_C. Because the speed is the first derivative of the displacement

$$V = \frac{dH}{dt}, \quad H(t=0) = 0. \tag{12}$$

The reached height about time in the phase of accelerating climb can be given by

$$H(t) = \int V(t)\, dt = \frac{1}{b^2} \ln\left[\exp(2abt) + 1\right] - \frac{a}{b} t, \quad t \in [0, t_{AC}]. \tag{13}$$

At the end of accelerating climb, the tailsitter reaches the height of $H_{AC} = H(t_{AC})$, which also depends on the expected constant climb velocity V_C.

2.2.2. Constant Velocity Climb. In the phase of constant velocity climb, ignoring wing-propeller interaction, the required thrust can be expressed as

$$T_C = W_{\mathrm{TO}} + \frac{\rho}{2} V_C^2 S C_{D0}. \tag{14}$$

As can be seen from (14), the higher the rate of climb V_C, the greater the thrust T_C needed. In view of the maximum thrust $T \le T_{\max}$, the maximum allowable rate of climb is

$$V_{\max} = \sqrt{\frac{2}{\rho C_{D0}}} \cdot \sqrt{K_T - 1} \cdot \sqrt{\frac{W_{\mathrm{TO}}}{S}}. \tag{15}$$

Given the aerodynamic and propulsion characteristics of a tailsitter, $V_{\max}$ would only depend on wing loading.

Because the tailsitter was driven by twin contrarotation propellers, as shown in Figure 1, each propeller needs to provide a half of the required thrust. The maximum operation power of each motor $P_{\mathrm{req}}^{\max}$ was determined by $T_{\max}$ and $V_{\max}$ through (6) as $P_{\mathrm{req}}^{\max} = P(k_T W_{\mathrm{TO}}/2, V_{\max})$. So the necessary mass of each motor-propeller system, including the propeller, the motor, and the ESC, could be expressed as

$$m_{\mathrm{EMP}} = K_{\mathrm{EMP}} P_{\mathrm{req}}^{\max}, \tag{16}$$

where K_{EMP} is the mass-power coefficient of the motor-propeller system in unit of kg/W.

2.2.3. Energy Consumption in Climb. The actual required power for each propeller in the phase of constant velocity climb is still calculated by the momentum theory as $P_C = P(T_C/2, V_C)$ by (6). The total energy consumption in the phase of constant climb for the tailsitter is

$$E_C = 2 \cdot \frac{P_C}{\eta_B \eta_E \eta_M} \frac{H_m - H_{AC}}{V_C}. \tag{17}$$

For accelerating climb, the required power for each propeller at any time $t \in [0, t_{AC}]$ is calculated similarly by (6) as $P_{AC}(t) = P(T_{\max}/2, V(t))$, where climb velocity $V(t)$ can be yielded by (11). So the energy consumption in the phase of accelerating climb could be given by integration:

$$E_{AC} = \frac{2 \int_0^{t_{AC}} P_{AC}(t)\, dt}{\eta_B \eta_E \eta_M}, \tag{18}$$

where the upper limit of the integration t_{AC} can be yielded by (10) with the constant climb velocity V_C. Then the total energy consumption for climb can be given by

$$E_{\mathrm{tot}} = E_{AC} + E_C. \tag{19}$$

Equation (19) is a high order nonlinear function about expected velocity V_C, which needs to be optimized within the feasible range $[0, V_{\max}]$ to minimize the energy consumption. The optimization problem can be written as follows:

$$\begin{aligned} &\text{find} && V_C \\ &\min && E_{\mathrm{tot}} \\ &\text{subject to} && 0 < V_C < V_{\max}. \end{aligned} \tag{20}$$

2.2.4. Power of Level Flight. For different flight missions, different level flight velocities V_{LF} could be adopted by a tailsitter for better performance. And then, different required thrusts T_{LF} and propeller efficiency result in the required power P_{LF} for level flight various. Considering two typical flight conditions, maximum range and endurance, the level flight performance of a battery powered tailsitter will be analyzed.

The steady level flight performance of a propeller-driven tailsitter could be estimated according to the literature [14]. When L/D and $C_L^{3/2}/C_D$ gain the maximum values at the flight conditions of $KC_L^2 = C_{D0}$ and $KC_L^2 = 3C_{D0}$, respectively, the maximum level flight range and endurance can be yielded, where $K = 1/\pi eAR$ and e is Oswald's efficiency which is set to 0.85 in this study because the wing configuration is nontapered and nonswept. The corresponding level flight velocities V_R and V_E can be deduced from the equality of the tailsitter's lift L and weight W_{TO} as

$$V_R = \sqrt{\frac{2W_{\mathrm{TO}}}{\rho S_{\mathrm{wing}}}\sqrt{\frac{K}{C_{D0}}}},$$
$$V_E = \sqrt{\frac{2W_{\mathrm{TO}}}{\rho S_{\mathrm{wing}}}\sqrt{\frac{K}{3C_{D0}}}}. \tag{21}$$

Required thrusts T_R and T_E can be yielded by the equality of the thrust and the drag acting on the tailsitter:

$$T_R = D_R = \frac{\rho}{2}V_R^2 S_{\mathrm{wing}} \cdot 2C_{D0},$$
$$T_E = D_E = \frac{\rho}{2}V_E^2 S_{\mathrm{wing}} \cdot 4C_{D0}. \tag{22}$$

For such two steady level flight conditions, power consumption of each propeller can be given by the momentum theory as $P_E = P(D_E/2, V_E)$ and $P_R = P(D_R/2, V_R)$.

2.2.5. Energy Consumption in Landing. Being subjected to structural constraints and landing quality requirements, the landing velocity of a tailsitter should be strictly restricted. The allowable landing loads for T-wing were a drop from 4.0-foot height [5], which meant a maximum allowable landing velocity of 4.88 m/s. Considering the stability of a descending tailsitter, the crucial elevons required a high dynamic pressure which was determined by the propellers' slip velocity and the descent velocity. So high propeller disk loading and a low descending velocity were recommended.

The induced velocity V_H at the propeller disk in hover is an important reference for the analysis of tailsitter descent, which could be expressed as

$$V_H = \sqrt{\frac{T_{\mathrm{hover}}}{2\rho A}} = \sqrt{\frac{W_{\mathrm{TO}}}{4\rho A}}. \tag{23}$$

As propeller radius $R_P = 0.25b_{\mathrm{wing}} = 0.25\sqrt{S \cdot AR}$, substituting propeller disk area $A = \pi R_P^2$ into (23) then we yield a more specific version of the reference velocity as

$$V_H = \sqrt{\frac{4k_{WS}}{\rho\pi AR}}. \tag{24}$$

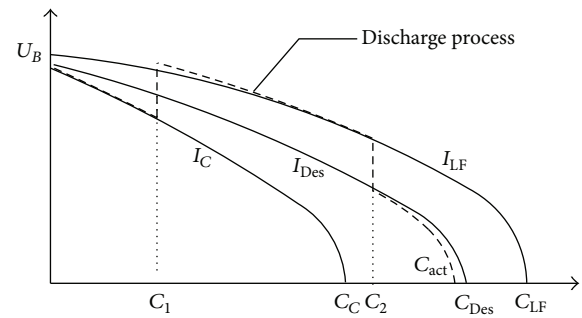

Figure 3: Illustration of the battery discharge process with variable current draw.

A descent velocity of $V_{\mathrm{Des}} = 4$ m/s was suggested in this paper, and then the propellers are working on a condition of low speed axial descent $V_{\mathrm{Des}} < 2V_H$. Assuming the variable $x = -V_{\mathrm{Des}}/V_H$, the actual induced velocity V_i at the propeller disk can be given by the quartic approximation [13]:

$$V_i = \left(\kappa - 1.125x - 1.372x^2 - 1.718x^3 - 0.655x^4\right)V_H. \tag{25}$$

And then, ignoring the aerodynamic forces on the wing, the required power of each propeller at such low rate of descent can be expressed as

$$P_{\mathrm{Des}} = \kappa T_{\mathrm{req}} V_{\mathrm{disk}} = \kappa W_{\mathrm{TO}}\left(V_i - V_{\mathrm{Des}}\right). \tag{26}$$

Therefore, the total energy consumption E_{Des} for vertical landing is

$$E_{\mathrm{Des}} = \frac{2\kappa W_{\mathrm{TO}}\left(V_i - V_{\mathrm{Des}}\right)H_m}{\eta_B\eta_E\eta_M V_{\mathrm{Des}}}. \tag{27}$$

2.3. Battery Discharge. For current rechargeable batteries, such as lithium-polymer battery, the effective capacity has a relationship with actual current draw as Peukert effect [15, 16]. The operation powers of the tailsitter for vertical climb, level flight, and vertical descent are different from each other, and there is $P_C > P_{\mathrm{Des}} > P_{\mathrm{LF}}$. With the same battery voltage level, the higher flight power leads to a higher current draw for each motor-propeller system, $I_C > I_{\mathrm{Des}} > I_{\mathrm{LF}}$, and a consequential less effective capacity $C_C < C_{\mathrm{Des}} < C_{\mathrm{LF}}$. Considering batteries' voltage drop actually, the discharge processes for climb, level flight, and descent are sketched in Figure 3, where C_C, C_{Des}, and C_{LF} represent the effective capacities corresponding to such three different current draws, respectively, and U_B is the nominal terminal voltage. As residual capacity could be utilized for further discharge [17], the actual flight discharge process is illustrated by dash lines, where C_1 represents the consumed capacity in climb, C_2 represents the total capacity that has discharged before descent, and C_{act} represents the total capacity of a full discharge process.

Theoretical calculation based on the assumption of constant battery voltage was carried out to estimate the possible level flight endurance as

$$t_{\mathrm{LF}} = \frac{C_2 - C_1}{2I_{\mathrm{LF}}} = \frac{C_{\mathrm{act}}}{2I_{\mathrm{LF}}} - \frac{C'_D + C'_C + C'_{AC}}{2I_{\mathrm{LF}}}, \tag{28}$$

where C'_D, C'_C, C'_{AC} represent the consumed capacity in descent, constant velocity climb, and accelerating climb and multiplication by two in the denominator represents the fact that such two motor-propeller systems are powered by the same battery pack. It can be deduced from the experiments [17] that $C_{\mathrm{act}} \approx C_{\mathrm{Des}}$, so there is

$$\begin{aligned} t_{\mathrm{LF}} &= \frac{C_{\mathrm{Des}}}{I_{\mathrm{Des}}} \cdot \frac{I_{\mathrm{Des}} U_B}{2I_{\mathrm{LF}} U_B} - \frac{\left(C'_D + C'_C + C'_{AC}\right) U_B}{2I_{\mathrm{LF}} U_B} \\ &= \frac{C_{\mathrm{Des}}}{I_{\mathrm{Des}}} \cdot \frac{P_{\mathrm{Des}}}{2P_{\mathrm{LF}}} - \frac{E_{\mathrm{Des}} + E_{\mathrm{tot}}}{2P_{\mathrm{LF}}}. \end{aligned} \tag{29}$$

Peukert equation tells that $C_B I_B^{n-1} = C_{\mathrm{Des}} I_{\mathrm{Des}}^{n-1}$, and $t_B = 1$ hour for small battery gives

$$\frac{C_{\mathrm{Des}}}{I_{\mathrm{Des}}} = \frac{C_B I_B^{n-1}}{I_{\mathrm{Des}}^n} = t_B^{1-n} \frac{C_B^n U_B^n}{I_{\mathrm{Des}}^n U_B^n} = \left(\frac{E_B}{P_{\mathrm{Des}}}\right)^n, \tag{30}$$

where E_B is the electric energy stored in battery; n is the Peukert coefficient; P_{LF} represents the maximum range power P_R or the maximum endurance power P_E. Considering the efficiency of energy transformation, the level flight endurance is

$$t_{\mathrm{LF}} = \left(\frac{m_B K_{\mathrm{BEm}} \eta_B \eta_E \eta_M}{P_{\mathrm{Des}}}\right)^n \frac{P_{\mathrm{Des}}}{2P_{\mathrm{LF}}} - \frac{E_{\mathrm{Des}} + E_{\mathrm{tot}}}{2P_{\mathrm{LF}}}, \tag{31}$$

where $m_B = k_B W_{\mathrm{TO}}/g$ is the mass of battery and K_{BEm} is the specific energy of battery.

3. Parameter Influence Study

For conventional battery powered airplane, the required power for level flight is

$$\overline{P_{\mathrm{LF}}} = \frac{C_D}{C_L^{3/2}} \sqrt{\frac{2}{\rho}} \sqrt{\frac{W_{\mathrm{TO}}^3}{S}}. \tag{32}$$

Generally, the propeller's efficiency was regarded as constant η_P that was independent of flight conditions; a total efficiency of BEMP propulsion system $\eta_{\mathrm{tot}} = \eta_B \eta_E \eta_M \eta_P$ could be used to evaluate the influence of wing loading and battery ratio on endurance performance as

$$\begin{aligned} \overline{t_{\mathrm{LF}}} &\approx \left(\frac{E_B \eta_{\mathrm{tot}}}{\overline{P_{\mathrm{LF}}}}\right)^n = \left(\sqrt{\frac{\rho}{2}} \frac{C_L^{3/2}}{C_D} \frac{k_B K_{\mathrm{BEm}} \eta_{\mathrm{tot}}}{g\sqrt{k_{WS}}}\right)^n \\ &\propto \left(\frac{k_B}{\sqrt{k_{WS}}}\right)^n. \end{aligned} \tag{33}$$

As can be seen from (33), there is a positive correlation between the endurance and battery ratio and a negative correlation between the endurance and wing loading.

Table 1: Parameters that are constant or assumed to be constant.

Parameter	Value	Unit	Description
k_A	0.1	—	Avionics weight ratio
k_F	0.2	—	Fuselage and strength structure weight ratio
k_W	20	$\mathrm{N/m^2}$	Wing weight coefficient
AR	5.0	—	Wing aspect ratio
C_{D0}	0.03	—	Wing zero-lift drag coefficient
K_{BEm}	150	Wh/kg	Battery specific energy
K_{EMP}	5×10^{-4}	kg/W	Mass-power coefficient of motor-propeller system
η_B	0.95	—	Efficiency of battery discharge
η_E	0.95	—	Efficiency of ESC
η_M	0.9	—	Efficiency of BLDC motor
n	1.3		Peukert coefficient for Li-Po battery
H_m	1000	m	Mission height
m_{PL}	1.0	kg	Mass of mission payloads

Simulations were carried out to examine the influence of wing loading and battery ratio on battery powered tailsitters' range and endurance performance.

3.1. Parameters. At the beginning of numerical analysis, it is necessary to distinguish former parameters and constraints between three different classes: constant or assumed constant parameters, design variables, and intermediate variables.

(1) *Parameters that are constant or assumed to be constant* are listed in Table 1, which are linked to the design experience of tailsitters [2], general level of current technology about wing structure [18], lithium-polymer (Li-Po) batteries, ESCs and BLDC motors [19], typical mission performance of small battery powered UAVs [20, 21], and so forth.

(2) *Design variables* are wing loading k_{WS} and ratio of battery weight k_B. It is known from (4) that $k_{WS} > k_W/(1 - k_A - k_F) = k_{WS}^0$ and $k_B < 1 - k_A - k_F - k_W/k_{WS} = k_B^0$. Analysis will focus on small tailsitters of $W_{\mathrm{TO}} < 20$ kg; therefore numerical approximations of $k_{WS} \geq 2k_{WS}^0$ and $k_B \leq 0.9k_B^0$ will be applied.

(3) *Intermediate variables* include the climb velocity V_C and the mass of motor-propeller system m_{EMP}, which need to be optimized, and powers and energy consumption of climb and descent, P_C, E_C, P_{Des}, and E_{Des}, which need to be evaluated.

3.2. Simulation Results

(1) Feasible Design Space. As can be seen from Figure 4, there are consistent left and right margins for Figures 4(a) and 4(b),

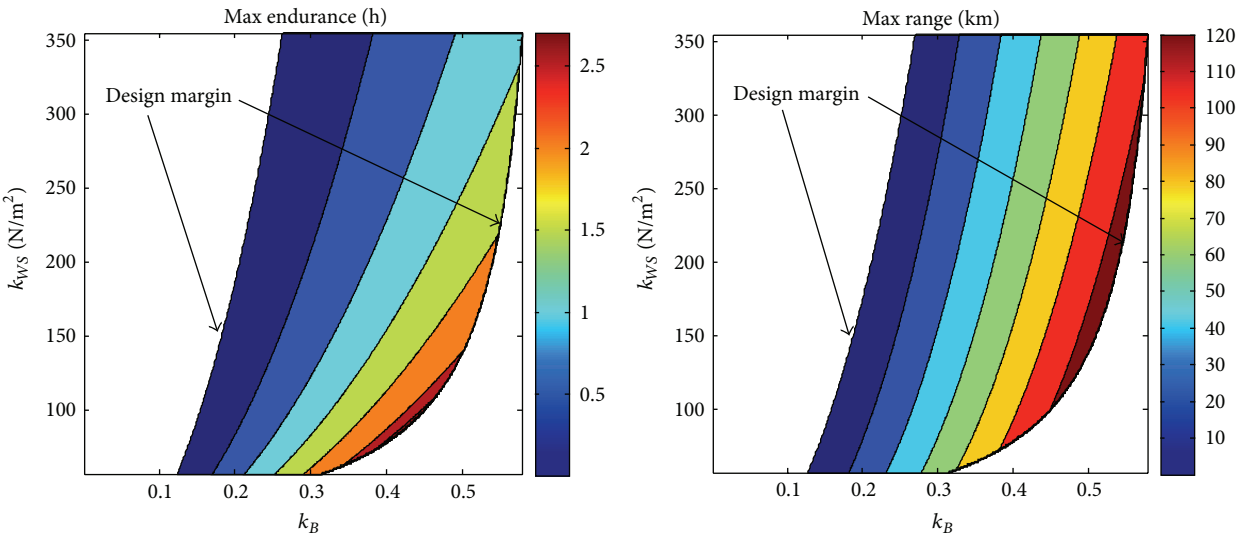

(a) $t_{\mathrm{LF}} > 0$ (b) Range > 0

Figure 4: Feasible design space about wing loading and battery ratio.

between which the feasible design space for battery powered tailsitters about wing loading and battery ratio is demonstrated. The left margin represents the minimum k_B for different k_{WS}, which means that carried battery could only support the tailsitter to vertically climb to the mission height and land back on the ground. There are $t_{\mathrm{LF}} = 0$ and range = 0 on the left margin. The theoretic right margin is determined by wing loading's lower limit k_{WS}^0 and battery ratio's upper limit k_B^0. Because numerical calculation could not reach such limits directly, Figure 4 shows a dynamic approximation of the theoretic right margin.

In feasible design space, the level flight range and endurance performance vary with k_B and k_{WS}. Both the optimum wing loading and battery ratio for maximum range, k_{WS}^R and k_B^R, are higher than the optimum values of k_{WS}^E and k_B^E for maximum endurance, respectively. Meanwhile, it can be deduced from Figure 4 that too small wing loading will not be proposed for better level flight performance. The reason is that a smaller k_{WS} leads to a smaller upper limit of battery ratio, while k_B plays a more important role in level flight performance improvement as (33) shows.

(2) Weight and Power Level. Takeoff weights for all possible designs based on possible wing loading and battery ratios are shown in Figure 5(a), and partly designs are unfeasible as battery energy could not support any level flight at the mission height. As $k_{WS} \to k_{WS}^0$ and $k_B \to k_B^0$, W_{TO} will increase quickly, and level flight endurance and range increase correspondingly as shown in Figure 4.

Optimization results indicate that the optimum constant climb velocity V_C^{opti} and the necessary weight ratio of motor-propeller system $k_{\mathrm{EMP}} = W_{\mathrm{EMP}}/W_{\mathrm{TO}}$ are only related to tailsitter's wing loading, as shown in Figure 5(b). Motor-propeller system weight increases gradually from less than 10 percent of W_{TO} to nearly 20 percent, while V_C^{opti} firstly increases and then decreases slightly as $k_{WS} > 300\,\mathrm{N/m^2}$.

Given the values of k_B and k_{WS}, for a determinate design of battery powered tailsitter in other words, the power of constant velocity climb P_C is approximately 10 times P_E, as the comparison shown in Figure 6. That is the significant distinction between the tailsitter and the CTOL UAVs. Optimizations on climb path and transition maneuver will be significant for tailsitter's performance improvement.

In summary, the wing loading and battery ratio of battery powered tailsitters should be optimized based on mission parameters for better level flight performance.

4. Preliminary Design Case

4.1. Design Method and Process. Being subjected to the constraints of allowable takeoff weight and maximum climb velocity, the optimum wing loading and battery ratio need to be determined, and the constant climb velocity should be optimized for maximum level flight endurance for given mission height and payloads. The design method for a small unmanned battery powered tailsitter could be summarized to an optimization problem, expressed as follows:

$$\begin{aligned} \max \quad & \text{endurance}\,(k_B, k_{WS}) \\ \text{subject to} \quad & W_{\mathrm{TO}} \le W_{\mathrm{allow}}, \\ & 0 < V_C < V_{\max}. \end{aligned} \tag{34}$$

The weight of the motor-propeller system W_{EMP} is determined by the maximum takeoff power $P_{\mathrm{req}}^{\max} = P(k_T W_{\mathrm{TO}}/2, V_{\max})$. Iterations are carried out with (4), (15), and (16) for an appropriate solution. The flowchart of the preliminary design process for battery powered tailsitters is shown in Figure 7.

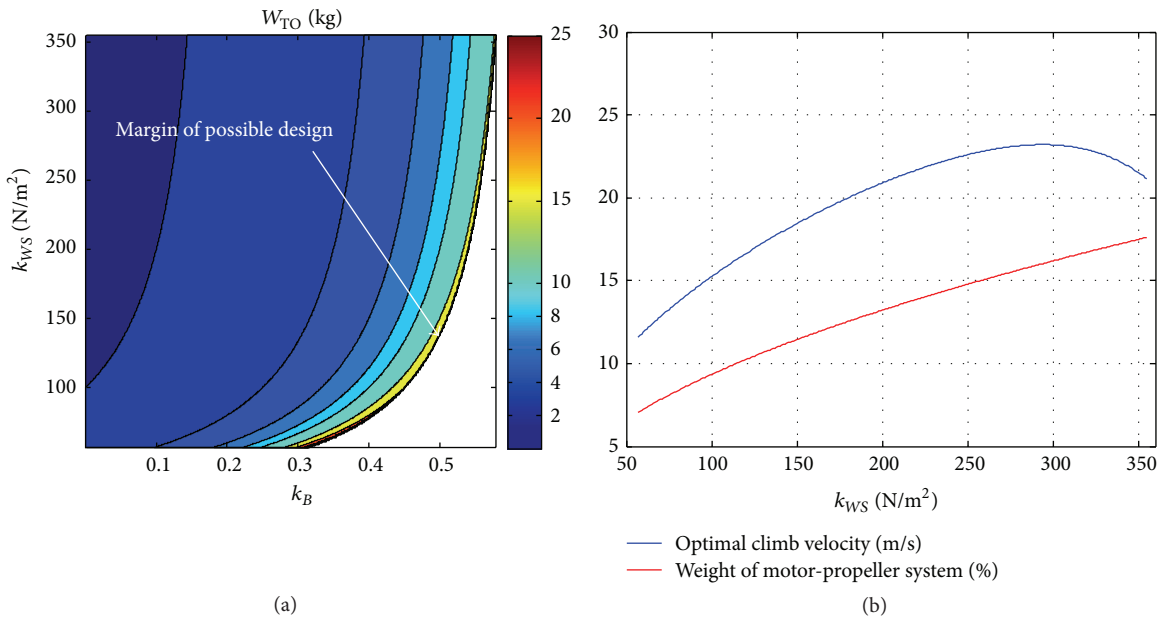

FIGURE 5: (a) Takeoff weight for all possible designs; (b) optimum constant climb velocity and motor-propeller system weight for different wing loading.

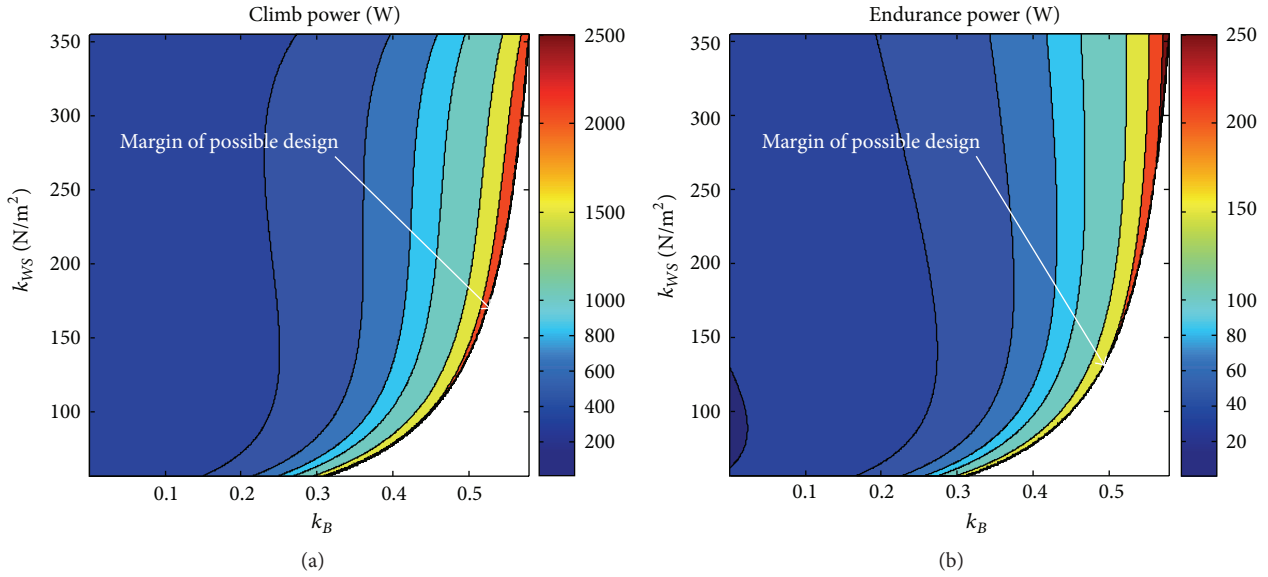

FIGURE 6: Power levels comparison between climb and maximum endurance level flight.

4.2. Results and Discussion. In order to examine the influences of mission parameters and design constraints, four mission heights, 250 m, 500 m, 750 m, and 1000 m, were introduced; allowable mass of the tailsitter was set to $3 \leq m_{TO} \leq 20$ kg. Other parameters were consistent with former simulation listed in Table 1. Maximum level flight endurance for different mission heights and allowable takeoff weights is shown in Figure 8. For the same mission height, level flight endurance increases when greater takeoff weight was allowed. But such increasing will slow down especially as $m_{TO} > 10$ kg. The maximum level flight endurance for a 10 kg battery powered tailsitter is about 2.792 hours while the mission height is 250 m. Lower mission height contributes to longer level flight endurance for an expected takeoff weight. When the mission height drops from 1000 m to 250 m, there is about 0.7 hours' extension with the allowable mass more than 10 kg. That is less obvious for small battery powered tailsitters lighter than 5 kg.

Correspondingly, Figures 9 and 10 show that the optimum values of wing loading and battery ratio decrease with mission height falling, while that is not very clear for small tailsitters as $m_{TO} < 5$ kg. For the same mission height, Figures 9 and 10 show that, with the greater allowable takeoff weight, the higher battery ratio and the smaller wing loading are necessary for optimum level flight endurance. It is not

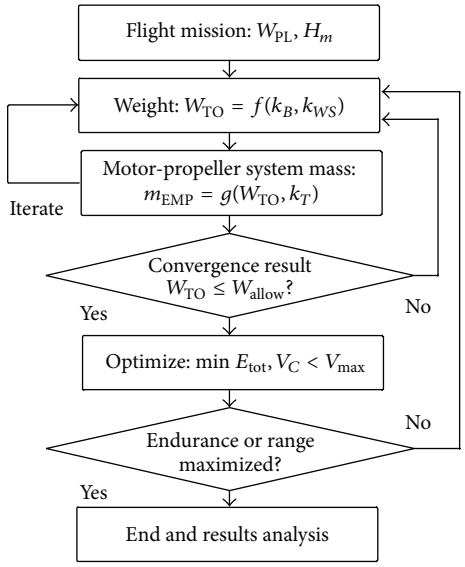

Figure 7: Flowchart of preliminary design for battery powered tail-sitters.

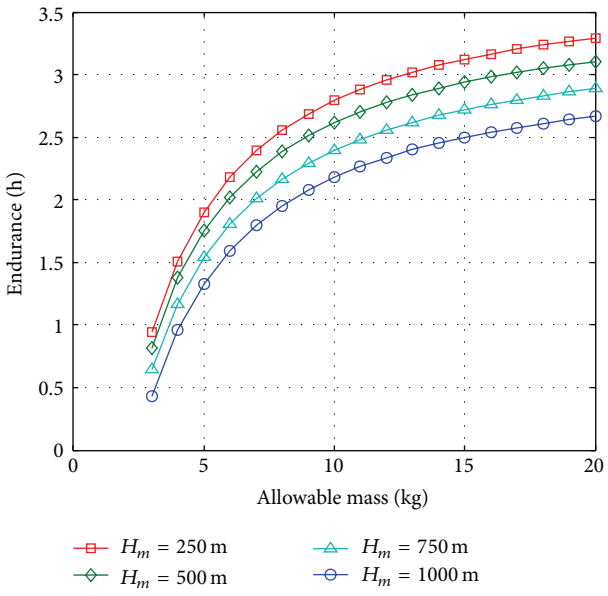

Figure 8: Maximum endurance for different mission heights and takeoff weights.

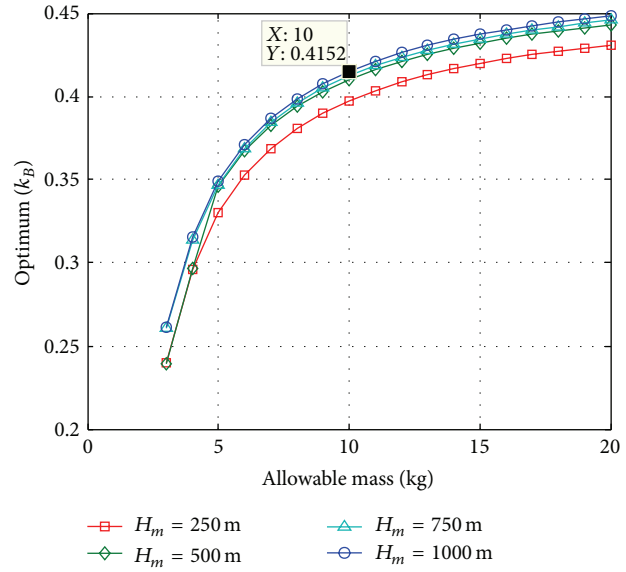

Figure 9: Optimum wing loading for different mission heights and takeoff weights.

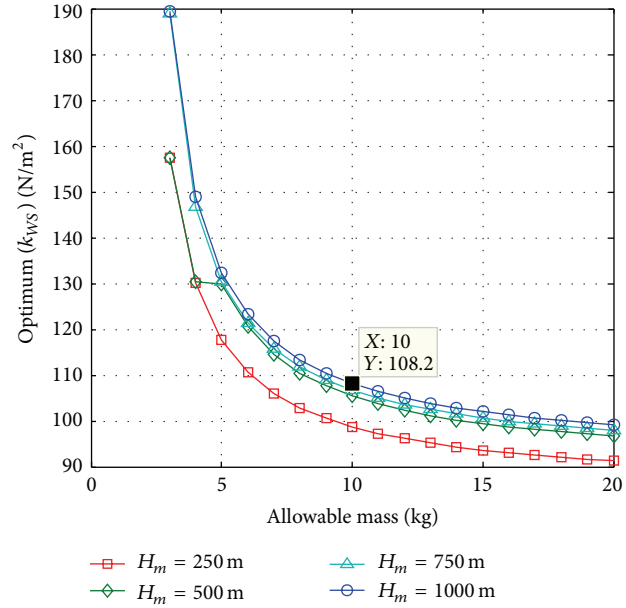

Figure 10: Optimum battery ratios for different mission heights and takeoff weights.

difficult to deduce from (4) that $k_B + k_W/k_{WS} = 1 - k_A - k_F - (W_M + W_{PL})/W_{TO}$, so greater W_{TO} means the feasible ranges of k_B and k_{WS} extend. A higher battery ratio and smaller wing loading are help for flight performance improvement, as demonstrated by Figure 4 and (33).

In order to validate the reasonability of the design result, design parameters and performance characteristics of four battery powered terrestrial UAVs were collected, as listed in Table 2, where electrical T-wing [22] (E-T-wing for short) and ITU-Tailsitter [7] are tailsitter configuration; TURAC [21] has a configuration of separate propulsion systems used for vertical flight and level flight, respectively; ITU-Tailless [20] is a CTOL UAV with flying wing configuration.

The E-T-wing demonstrator vehicle was powered by 9.1 kg Ni-Cd batteries, the specific energy of which is 110 J/g, approximately 396 Wh/kg. Except for the problems with motor speed controllers induced unreliability [5], there might be other problems leading to the electrical powered scheme cancelled. These problems might involve heavy takeoff weight causing too heavy wing loading and small diameter (less than 0.6 m) propellers causing inefficient propulsion. High power operations, 3.138 kW for hover and 1.021 kW for level

Table 2: Parameters and performances of four battery powered UAVs.

Items	E-T-wing	ITU-Tailsitter	TURAC	ITU-Tailless
Takeoff	VTOL	VTOL	VTOL	CTOL
W_{TO} (kg)	22.72	10.0	47.0	7.74
W_{PL} (kg)	1.8	1.0	8.0	1.3
H_m (m)	1 min[†]	1000	1000	250
AR	6.47	5.78	5.25	8.89
C_{D0}	0.048	—[#]	0.0266	0.033
k_{WS} (N/m^2)	304.3	196.0	137.1	99.8
k_B	0.4004	—[#]	0.468	0.3876
t_{LF} (h)	≤0.1	≈2.0	≈1.5	≈3.0

[†]Mission height is not known, while 1 minute vertical flight has been mentioned [5].
[#]Data could not be obtained by open literatures.

flight, not only cause batteries' discharge duration reduced, but also lead to effective battery capacity reduced caused by high current draw [15].

Both ITU-Tailsitter and TURAC employed separate-dual propulsion system, independent propulsion for vertical takeoff and landing in other words, which introduced dead weight for level flight inevitably. As (33) presented, heavy wing loading listed in Table 2 was not help for endurance performance improvement. CTOL ITU-Tailless was listed for comparison. Hand-launch could reduce takeoff energy consumption and large aspect ratio wing leads to better aerodynamic performance, so the level flight duration is much longer.

Carrying 1.0 kg payloads, the optimization designed 10 kg unmanned battery powered tailsitter has level flight endurance of 2.18 hours at the mission height of 1000 m, a comparative performance of ITU-Tailsitter. Meanwhile, Figures 9 and 10 show that the corresponding optimum wing loading and battery ratio are $k_{WS} = 108.2\,\text{N/m}^2$ and $k_B = 0.4152$, respectively. The energy consumption of avionics and other instruments needs to be counted in further study for more precise endurance estimation.

5. Summary and Conclusion

Focusing on the level flight performance, this paper simplified the design process of battery powered tailsitters. A complete flight profile for small unmanned tailsitters has been established and detailedly discussed phase by phase, which set a basic reference for tailsitter's flight path optimization. The feasible design space and illustrated design method, as well as the power level and energy consumption of each flight phase, can be used to provide guidance for the tailsitter's detailed design. Although the design methodology was initially intended for terrestrial UAVs, that can be also adapted for Martian tailsitters with the considering of environment parameters and flight missions.

Competing Interests

The authors declare that there are no competing interests regarding the publication of this paper.

Acknowledgments

The authors would like to acknowledge the support provided by the Aeronautical Science Foundation of China under Grant no. 20145788006.

References

[1] W. Graham, "Google details 'Project Wing' unmanned package-delivery R&D," in *Aviation Week & Space Technology*, 2014.

[2] J. L. Forshaw and V. J. Lappas, "Architecture and systems design of a reusable Martian twin rotor tailsitter," *Acta Astronautica*, vol. 80, pp. 166–180, 2012.

[3] L. A. Young, E. Aiken, P. Lee, and G. Briggs, "Mars rotorcraft: possibilities, limitations, and implications for human/robotic exploration," in *Proceedings of the IEEE Aerospace Conference*, Big Sky, Mont, USA, 2005.

[4] L. A. Young and E. W. Aiken, "Vertical lift planetary aerial vehicles: three planetary bodies and four conceptual design cases," in *Proceedings of the 27th European Rotorcraft Forum*, Moscow, Russia, 2001.

[5] R. H. Stone, *Configuration design of a canard configured tail sitter unmanned air vehicle using multidisciplinary optimization [Ph.D. thesis]*, University of Sydney, 1999.

[6] K. C. Wong, J. A. Guerrero, D. Lara, and R. Lozano, "Attitude stabilization in hover flight of a mini tail-sitter UAV with variable pitch propeller," in *Proceedings of the IEEE/RSJ International Conference on Intelligent Robots and Systems (IROS '07)*, pp. 2642–2647, IEEE, San Diego, Calif, USA, November 2007.

[7] M. Aksugur and G. Inalhan, "Design methodology of a hybrid propulsion driven electric powered miniature tailsitter unmanned aerial vehicle," *Journal of Intelligent and Robotic Systems*, vol. 57, no. 1–4, pp. 505–529, 2010.

[8] D. Kubo, K. Muraoka, N. Okada, M. Naruoka, T. Tsuchiya, and S. Suzuki, "Flight testing of a wing-in-propeller-slipstream mini unmanned aerial vehicle," in *Proceedings of the AIAA Infotech@Aerospace Conference*, AIAA Paper 2009-2070, Seattle, Wash, USA, April 2009.

[9] C. D. Wagter, D. Dokter, G. D. Croon, and B. Remes, "Multi-lifting-device UAV autonomous flight at any transition percentage," in *Proceedings of the European Guidance, Navigation, and Control Conference (EuroGNC '13)*, Delft, The Netherlands, 2013.

[10] P. Sinha, P. Esden-Tempski, C. A. Forrette, J. K. Gibboney, and G. M. Horn, "Versatile, modular, extensible VTOL aerial platform with autonomous flight mode transitions," in *Proceedings of the IEEE Aerospace Conference*, Big Sky, Mont, USA, March 2012.

[11] R. H. Stone, "The T-wing tail-sitter unmanned air vehicle: from design concept to research flight vehicle," *Proceedings of the Institution of Mechanical Engineers, Part G: Journal of Aerospace Engineering*, vol. 218, no. 6, pp. 417–433, 2004.

[12] M. Gatti, F. Giulietti, and M. Turci, "Maximum endurance for battery-powered rotary-wing aircraft," *Aerospace Science and Technology*, vol. 45, pp. 174–179, 2015.

[13] J. G. Leishman, *Principles of Helicopter Aerodynamics*, Cambridge University Press, New York, NY, USA, 2006.

[14] J. D. Anderson, *Aircraft Performance and Design*, WCB/McGraw-Hill, Bethesda, Md, USA, 1999.

[15] L. W. Traub, "Range and endurance estimates for battery-powered aircraft," *Journal of Aircraft*, vol. 48, no. 2, pp. 703–707, 2011.

[16] G. Avanzini and F. Giulietti, "Maximum range for battery-powered aircraft," *Journal of Aircraft*, vol. 50, no. 1, pp. 304–307, 2013.

[17] D. Doerffel and S. A. Sharkh, "A critical review of using the Peukert equation for determining the remaining capacity of lead-acid and lithium-ion batteries," *Journal of Power Sources*, vol. 155, no. 2, pp. 395–400, 2006.

[18] X. Zhu, Z. Guo, R. Fan, Z. Hou, and X. Gao, "How high can solar-powered airplanes fly," *Journal of Aircraft*, vol. 51, no. 5, pp. 1653–1658, 2014.

[19] B. Wang, Z. Hou, and W. Wang, "Performance analysis of propulsion system of miniature electric-powered vertical takeoff and landing air vehicles," *Journal of National University of Defense Technology*, vol. 37, no. 3, pp. 84–90, 2015 (Chinese).

[20] H. Karakas, E. Koyuncu, and G. Inalhan, "ITU tailless UAV design," *Journal of Intelligent and Robotic Systems: Theory and Applications*, vol. 69, no. 1–4, pp. 131–146, 2013.

[21] U. Ozdemir, Y. O. Aktas, A. Vuruskan et al., "Design of a commercial hybrid VTOL UAV system," *Journal of Intelligent & Robotic Systems*, vol. 74, no. 1-2, pp. 371–393, 2014.

[22] R. H. Stone and G. Clarke, "The T-wing: a VTOL UAV for defense and civilian applications," in *Proceedings of the UAV Australian Conference*, Melbourne, Australia, 2001.